BIOCHEMISTRY

 Volume 44, Number 36 September 13, 2005

Articles

Asymmetric Distribution of Cooperativity in the Binding Cascade of Normal Human Hemoglobin. 1. Cooperative and Noncooperative Oxygen Binding in Zn-Substituted Hemoglobin†

Jo M. Holt, Alexandra L. Klinger,‡,§ Connie S. Yarian,‡,|| Varsha Keelara, and Gary K. Ackers*

Department of Biochemistry & Molecular Biophysics, Washington University School of Medicine, 660 South Euclid Avenue Box 8231, St. Louis, Missouri 63110

Received April 18, 2005; Revised Manuscript Received June 8, 2005

ABSTRACT: The complete binding cascade of human hemoglobin consists of eight partially ligated intermediates and 16 binding constants. Each intermediate binding constant can be evaluated via dimer−tetramer assembly when ligand configurations within the tetramer are fixed through the use of hemesite analogs. The Zn/Fe analog, in which the nonbinding Zn^{2+} heme substitutes for deoxy Fe^{2+} heme, also permits direct measurement of O_2 binding to the remaining Fe^{2+} hemesites within the symmetrically ligated Hb tetramers. Measurement of O_2 binding over a range of Zn/Fe Hb concentrations to both α-subunits (species ***23***) or to both β-subunits (species ***24***) shows noncooperative binding and incomplete saturation of the available Fe^{2+} hemesites. In contrast, the asymmetrically ligated Zn/FeO_2 species ***21***, in which both oxygens are bound to one of the dimers within the tetramer, exhibits positive cooperativity and >90% ligation under atmospheric conditions. These properties are confirmed in the present study by measurement of the rate constant for tetramer dissociation to free dimer. The binding constants thus derived for these partially ligated intermediates are consistent with the stoichiometric constants measured for native hemoglobin by standard O_2 binding techniques, providing additional evidence that Zn^{2+}-heme substitution provides an excellent deoxy hemoglobin analog. There is no evidence that Zn-substitution stabilizes a low-affinity form of the tetramer, as previously suggested. These characterizations demonstrate distinct, nonadditive physical properties of the doubly ligated tetrameric species, yielding an asymmetric distribution of cooperativity within the cascade of O_2 binding by human hemoglobin.

Human hemoglobin (Hb)[1] binds and delivers O_2 with positive cooperativity, generating eight partially ligated intermediates with different configurations of bound ligand among the four hemesites (Figure 1). Unique values for the binding constants of each intermediate tetramer, or microstate, are not accessible by analysis of traditional O_2 binding curves (*1*). To address this problem, a method was developed based on linkage thermodynamics, capitalizing on the correlation between O_2 binding constants and $\alpha\beta$ dimer → $\alpha_2\beta_2$ tetramer assembly constants (*2*). To apply this strategy to human Hb, it is necessary to fix the configuration of bound ligand in the tetramer, and this is accomplished through the use of nonlabile hemesite analogs (*3*). The

† This work was supported by grants from the National Institutes of Health (GM24486) and the National Science Foundation (MCB0077596).

* Author to whom correspondence should be addressed. E-mail: ackers@wustl.edu. Phone: 314-362-4406. Fax: 314-747-3467.

‡ These authors contributed equally to this work.

§ Current address: 3D Pharmaceuticals/Johnson & Johnson, Yardley, PA.

|| Current address: Qiagen, Los Angeles, CA.

[1] Hb, hemoglobin; HbA_0, normal adult human hemoglobin; Hp, haptoglobin.

10.1021/bi050709o CCC: $30.25
Published on Web 08/16/2005

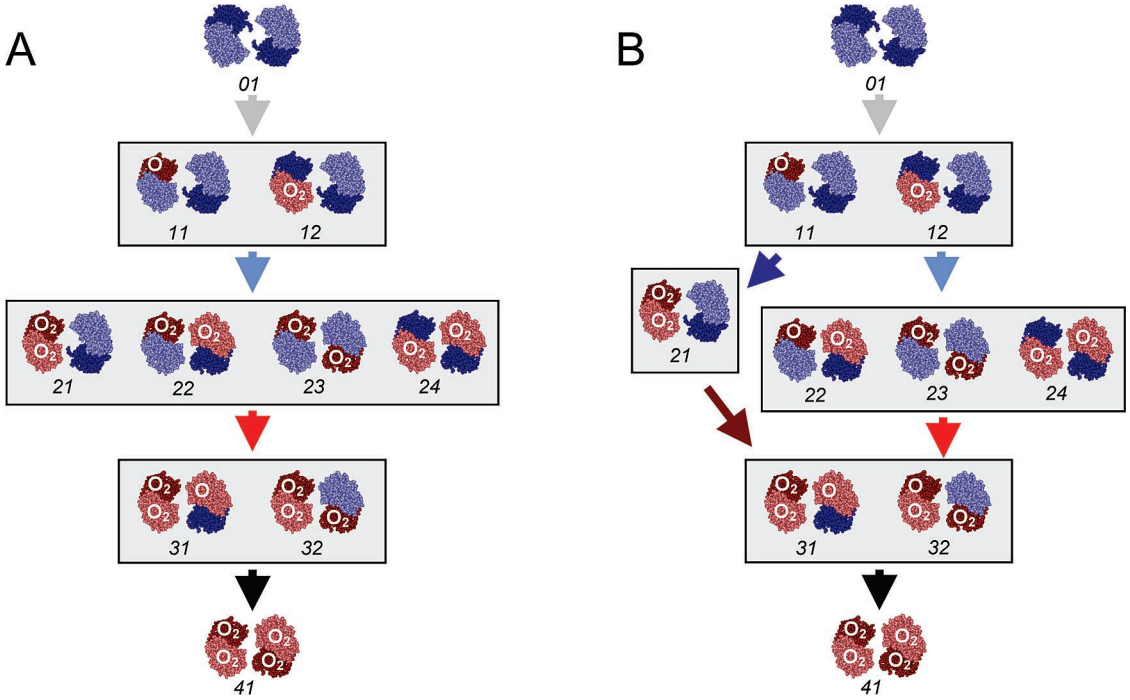

FIGURE 1: Oxygen binding cascade of human Hb. Deoxy subunits (blue) and oxy subunits (red) are further distinguished by α-subunits (dark shades) and *β*-subunits (light shades). Tetramer structures (*8*, *9*) are positioned looking down the central cavity from the *β*-cleft, and are shown in an exploded view to distinguish the two α*β* dimers. The eight intermediates have *i* ligands in distribution *j* among the four hemesites: the *ij* species designation is given below each Hb species depicted. The complete cascade from the deoxy tetramer to the fully liganded tetramer comprises a total of 10 unique pathways: four different pathways pass through species ***21***, four pass through species ***22***, one passes through species ***23***, and one passes through species ***24***. (A) Symmetric distribution of binding constants, in which the doubly ligated intermediates are assigned similar binding constants. This distribution is compatible with two-state models. (B) Experimentally determined distribution of binding constants, reflecting the configuration of bound ligand in each dimer within the Hb tetramer. Conditions are pH 7.4, 21.5 °C, 0.1 M Tris, 1 mM EDTA, and 0.18 M Cl^-.

sixteen constants so characterized provide a quantitative description of the entire binding cascade, which can be expressed in terms of assembly constants, ${}^{ij}\Delta G_2$, ligand binding constants, ΔG_{ij} , or the preferred term, cooperative free energy, ${}^{ij}\Delta G_c$ (as reviewed in refs *1* and *3*). This strategy has been applied using several hemesite analog systems, in differing solution conditions, and with both symmetric and asymmetric mutation or chemical modification. The primary findings can be summarized in two model-independent observations.

First, cooperativity is manifested between the α- and *β*-subunits within an α*β* dimer (*3*, *4*). This is most evident at the second binding step, where binding two ligands to the same α*β* dimer (to form species ***21***) is approximately 10-fold more favorable than binding one ligand to each deoxy α*β* dimer (to form species ***22***, ***23***, or ***24***) (Figure 1). Kinetic analysis of CO rebinding is also consistent with the equilibrium observation, in both wild type (*5*) and Co^{2+}-substituted Hb (*6*).

Second, cooperativity within one α*β* dimer can be modified independently of the partner α*β* dimer (*7*). Studies in which the tetramer is asymmetrically modified in the interfacial region between the two α*β* dimers (Figure 2) show that only the dimer bearing the modification exhibits a change in ligand binding constant: the wild type partner dimer still binds with the wild type constant, in the presence of a weakened dimer−dimer interface. The change in the modified dimer binding constant is equivalent to the change observed in the doubly modified tetramer.

Thus, the ligation-induced asymmetry present within the Hb tetramer is manifested as an asymmetric distribution of binding constants and, therefore, also of cooperativity, among the tetramers that comprise the binding cascade.

In model-based terms, cooperativity in human Hb has been traditionally attributed to the ligand-driven rearrangement of hydrogen bonding in the interface between the two α*β* dimers in the quaternary T ⇌ R switch. However, the microstate studies show overall cooperativity in Hb to be a combination of both intradimer (or tertiary) and cross-dimer (or quaternary) cooperativity. Furthermore, the observation that the cross-dimer strength can be weakened by modification without resulting in a significant change in intradimer cooperativity (on the wild type dimer) demonstrates an intradimer response to the perturbation that has always been interpreted in terms of a quaternary or cross-dimer response. Taken in sum, these data point to a greatly diminished role of quaternary effects in Hb cooperativity.

The previous success of models which rely on a single structural component to generate cooperativity in the Hb tetramer, i.e., the quaternary T ⇌ R switch, has been due in large part to two factors: (1) the reliance on stoichiometric O_2 binding constants or overall Hill coefficients to measure cooperativity and (2) the assumption of symmetry in the functional and structural responses of the Hb tetramer to perturbations. With regard to the first factor, direct O_2 binding to all four hemesites yields four stoichiometric constants, each of which is a composite of microstate constants rather than the individual microstate constants themselves (*1*). The

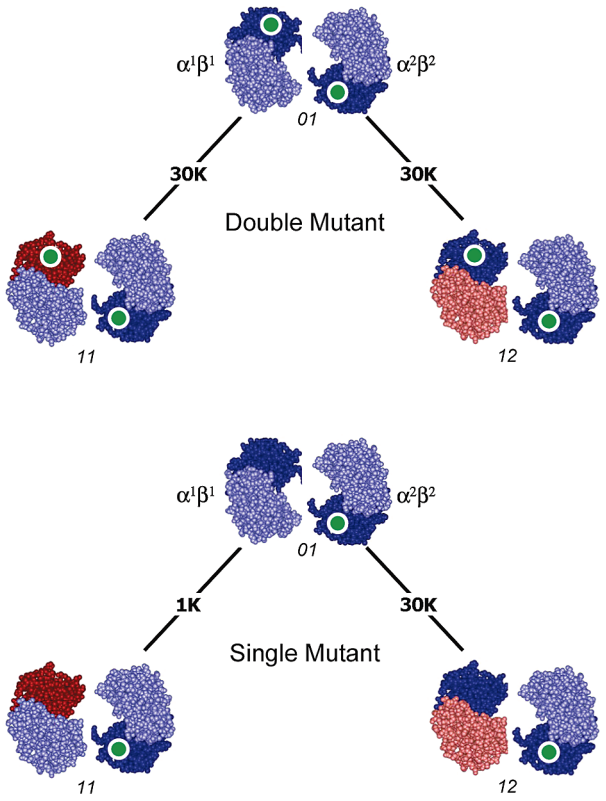

FIGURE 2: A single-site mutant of human Hb is normally modified in both α- or both *β*-subunits, thereby creating a "double" mutant (the mutation is indicated by a green dot, ligated subunits are red). In this example, the modified tetramer exhibits an increased O_2 affinity and increased dissociation to free dimer. These alterations in functional properties are also observed for the hybrid tetramer in which only one dimer carries the modification. However, microstate analysis shows that the enhanced affinity is due only to the modified dimer.

overall O_2 isotherm is dominated by the two end-states, a fact that is demonstrated by the ability to fit the experimental isotherms with a variety of two-state models (reviewed in ref *1*). These models predict that the properties of the partially ligated tetramers will be essentially additive combinations of the properties of the end-states, which is exactly what analysis of the O_2 binding curves reports. The contributions of the low-abundance partially ligated intermediates, which reveal nonadditive behavior, are largely hidden in the cooperative nature of the O_2 binding isotherm.

The second factor, an assumption of symmetry, is a critical element in models which limit the responses of the molecule to either T or R, and is built into the experimental design of the great majority of studies of Hb cooperativity. Thus, perturbations to Hb have almost exclusively been made simultaneously to both α*β* dimers, i.e., mutation, chemical modification, change in pH, addition of organic phosphate. The assumption of a symmetrical response to these perturbants by both α*β* dimers lends itself to a strictly quaternary interpretation of the observed effect on cooperativity. It is not until the tetramer is probed asymmetrically (on only a single subunit) that intradimer responses can begin to be deconvolved from cross-dimer responses (*7*).

These issues illustrate the importance of studying Hb at the microstate level, specifically, the partially ligated equilibrium states of the tetramer. To stabilize these intermediates, hemesite analogs are employed which must inevitably confer some structural and/or energetic artifact upon the system. It is then necessary to distinguish between a newly discovered property of Hb cooperativity and a hemesite analog artifact. The approach to this problem has been to measure microstate binding using a range of hemesite analogs with differing characteristics, and to apply all analogs to each of the possible combinatorial ligation intermediates (*1, 3*). The *consensus partition function* that has emerged describes the distribution of binding free energy throughout the Hb cascade (Figure 1) that is common to the entire microstate database. These consensus microstate binding constants generate an O_2 binding isotherm that is indistinguishable from the experimentally determined macro-binding curve (*1*). The effect of hemesite substitution itself is then minimized.

One surrogate heme, the Zn/Fe analog which employs the nonbinding Zn^{2+} heme as a deoxy hemesite analog, exhibits microstate binding constants that are the same as the consensus microstate constants (*4, 10, 11*). In addition, with this analog it is possible to measure direct O_2 binding to form symmetric species (e.g., species ***23*** and ***24***). In the present study, measurement of O_2 binding isotherms over a range of Zn/Fe Hb concentration is reported for species in which Zn^{2+} heme has been substituted in both α-subunits (species ***24***) or in both *β*-subunits (species ***23***). Consistent with a previous report by Noble and co-workers (*12*), binding to these microstate species is found to be incomplete and noncooperative. This finding is in contrast to that for the asymmetrically ligated Zn/FeO_2 species ***21***, in which both ligands are bound to one dimeric half-tetramer. Although direct O_2 binding to the asymmetric doubly ligated species ***21*** (as well as to other asymmetric microstates) is not experimentally feasible, sub-zero isoelectric focusing has permitted the dimer → tetramer equilibrium constant to be determined by thermodynamic linkage (*4, 13*). In the present study, the corresponding dissociation rate constant for the Zn/FeO_2 species ***21*** tetramer is measured, confirming the sub-zero focusing results which show positive cooperativity in binding both ligands to form species ***21***. Present results demonstrate that the two Fe-subunits within species ***21*** are fully ligated, in contrast with species ***23*** and ***24***. These characterizations provide further evidence for distinct, non-additive physical properties of the doubly ligated species. The properties of incomplete ligation and noncooperativity observed in the symmetric species ***23*** and ***24*** are also observed in the cooperative free energies of the other hemesite analogs, and are not artifacts of Zn^{2+} heme substitution, as addressed in the companion paper (*14*). Thus, specific binding sequences may vary in cooperativity within the highly cooperative cascade of O_2 binding by human Hb.

MATERIALS AND METHODS

Standard solution conditions used in the O_2 binding and stopped-flow kinetic studies reported here were 21.5 ± 0.2 °C in 0.1 M Tris, 0.1 M NaCl, 1 mM Na_2EDTA (SigmaUltra, Sigma/Aldrich) titrated to pH 7.4 to give a total [Cl^-] of 0.18 M. Deoxygenation procedures were carried out with humidified ultrahigh purity N_2 further purified by O_2-removing cartridges (QC+ panel/Agilent Technologies, Supelco), delivered in stainless steel or copper tubing (Swagelok). Temperature was controlled during all incubations and spectroscopic measurements by external water bath

(Neslab), monitored by calibrated thermocouples (YSI Inc., Yellow Springs, OH).

Preparation of Zn-Substituted Hemoglobin Tetramers

HbA_0 was purified from normal adult human blood by hemolysis with distilled water, followed by cation exchange chromatography with HPSP Sephadex (Amersham) (*13*). The α and β chains (containing the native Fe^{2+} heme) were prepared from the HbA_0 tetramer by reaction with ρ-hydroxymercuribenzoate, followed by purification using ion exchange chromatography and subsequent regeneration of sulfhydryl groups with β-mercaptoethanol (*13*). The α and β globins (without heme) were prepared from the HbA_0 tetramer by acid−acetone precipitation, followed by ion exchange chromatography. Chains containing Zn hemes were prepared from α globin by reconstitution with a molar excess of Zn^{2+}PPIX (Frontier Scientific, Logan, UT), followed by purification. Similar reconstitution with β globin gave poor yields of Zn β chains, as previously noted (*15*). To prepare species ***23*** (the tetramer in which β subunits contain Zn heme), β globin was mixed with Fe α chains to form a semiglobin, to which Zn^{2+}PPIX was added. To prepare species ***24*** (the tetramer in which α subunits contain Zn heme), Zn α chains were mixed with Fe β chains. Hybrid tetramers were purified by cation exchange chromatography (SP Sephadex) following assembly.

All modified tetramers were analyzed by electrospray mass spectometry (Protein and Nucleic Acid Laboratory, Washington University) to verify their molecular weights; purity was verified by the presence of a single band on isoelectric focusing (Pharmacia Phast System with ampholytes 6.7−7.7). Preparations involving Zn^{2+}PPIX were performed under red light (*16*). Millimolar extinction coefficients were obtained by titration of β93 cysteine sulfhydryl groups (*17*) for deoxy hybrid species ***23u*** ($\epsilon_{550} = 13.90$ and $\epsilon_{424} = 181.8$) and deoxy species ***24u*** ($\epsilon_{550} = 16.98$ and $\epsilon_{424} = 238.3$ mM^{-1} cm^{-1}). These parameter values are in agreement with previous reports (*15, 18*).

*Oxygen Binding To Form Symmetric Species **23** and **24***

Oxygen binding to form species ***23*** and ***24*** Zn^{2+}/Fe^{2+} hybrids was measured at a series of Hb concentrations. For concentrations <20 μM in heme, isotherms were obtained using a spectrophotometric apparatus based on the design of Imai (*19*) in the presence of an enzyme reductase system to maintain reduced heme Fe (*20*). Absorbance spectra were measured every 20 s throughout the deoxygenation process, from 600 to 500 nm at 1 nm intervals using a Varian Cary 4 spectrophotometer in rapid scanning mode (900 nm/min). Fractional saturation of each Hb sample was determined from spectra measured in the Imai cell as a function of O_2 concentration by normalizing with respect to the total change in absorbance at each wavelength.

Measurements conducted at higher concentrations employed a membrane-covered thin-layer optical cell based on the design of Gill (*21, 22*). The cell's dilution factor was determined by O_2 electrode to be 0.59 ± 0.005. Hb sample absorbances at 430 nm were monitored as a function of time during experiments. Absorbance traces showed characteristics typical for this technique, comprising a series of steps and plateaus. These raw data were transformed into fractional saturation curves by determining the average absorbance value, A, at each plateau, and normalizing to yield fractional O_2 saturation $\bar{Y}$:

$$\bar{Y} = \frac{(A - A_0)}{(A_\infty - A_0)} \quad (1)$$

where A_0 and A_∞ are upper and lower endpoint estimates. These parameters were allowed to vary in global nonlinear regression analyses of the isotherms using least squares criteria. The O_2 partial pressure at each dilution step was calculated as

$$(pO_2)_i = (pO_2)_0 r' \quad (2)$$

where pO_2 is the partial pressure of O_2 at the ith and 0th dilution steps and r' is the ratio of volumes for the sample compartment and dilution valve. Oxygen molarities in solution were calculated from partial pressures by Henry's Law, $[O_2] = (K_H)(pO_2)$, where K_H is the Henry's Law solubility constant, 1.78×10^{-6} M/Torr under these conditions (*23*).

Analysis of Binding Isotherms

Regression analysis was performed with the nonlinear least squares fitting program NONLIN (*24*). Binding isotherms were fit globally as a function of total protein concentration in order to rigorously account for O_2 binding to the dissociated dimers, as well as to the tetramers present in each sample. The fitting equations were thus formulated to account for the ligand-linked dimer to tetramer equilibrium reactions of Figure 3. Fitting functions and their derivations are given in the Supporting Information. Analysis requires the deoxy assembly constant, which is the value for the unligated species ***23*** or ***24*** (i.e., species ***23u*** or ***24u***), and was measured by haptoglobin trapping kinetics (*10*). Error estimates for all fitted parameters corresponded to a 65% confidence interval in a random system (*24, 25*).

In a small subset of experiments, corrections were made for deviations from ideal isosbestic point behavior by constraining the change in absorbance at each of the five isosbestic points in this wavelength range to zero. Using this constraint, a first order correction curve was calculated for each wavelength as a function of $[O_2]$. These corrections were small (<2% of the total absorbance change) and generally linear with respect to ln $[O_2]$. The normalized isotherms which had been wavelength dependent prior to this correction were indistinguishable after correction. Although numerical fitting of the uncorrected isotherms yielded parameter values identical to those of the corrected isotherms, the corrections served to eliminate systematic residuals.

It was observed that reactions with species ***23*** were distinctly less stable than those with species ***24***, and that great care had to be taken to avoid partial subunit denaturation and sample photodegradation in the Imai cell experiments, i.e., by reducing the stirring rate and monitoring O_2-dependent spectra only in the 500−600 nm region to minimize Zn heme photodegradation that can occur over 1−2 h at 470 nm in the presence of O_2. These small adjustments in procedure were essential for obtaining consistent results between the Imai cell (dilute) and Gill cell (concentrated) experiments.

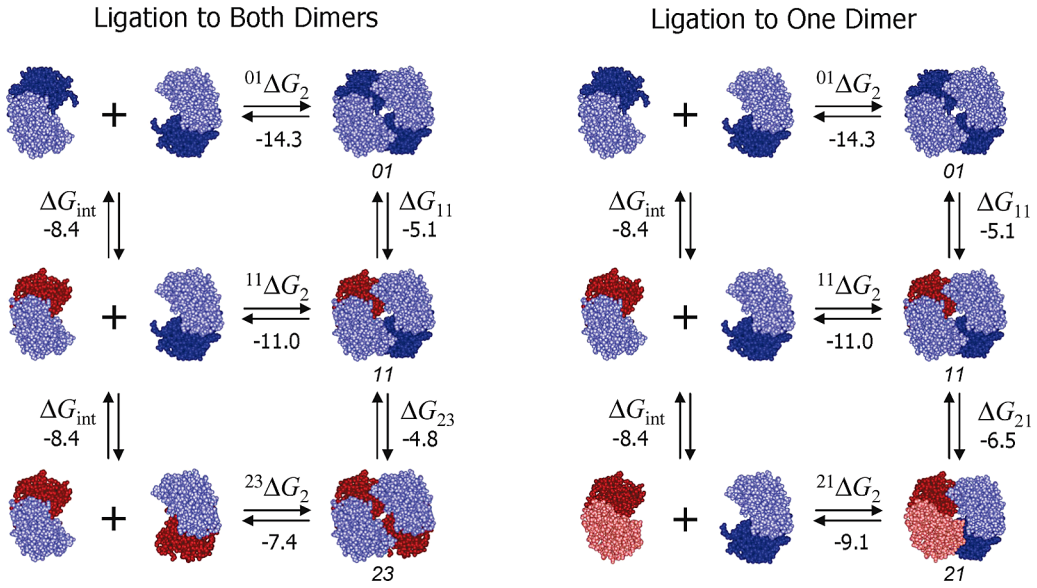

FIGURE 3: Dimer to tetramer assembly free energy ($^{ij}\Delta G_2$) is thermodynamically linked to oxygen binding free energy (ΔG_{ij}) in human Hb, illustrated here for the first two binding steps. Binding to the free dimer is noncooperative, and is assigned as the intrinsic binding free energy, ΔG_{int}. As ligation proceeds, the assembly free energy becomes less negative. Likewise, upon assembly of two free dimers to form one tetramer, the ligand binding free energy becomes less negative. The change in assembly free energy upon binding a ligand is equal to the change in ligand binding free energy upon assembly of dimer to tetramer (due to the path independence of free energy change), and is labeled the *cooperative free energy*, $^{ij}\Delta G_c$. Cooperative free energy reflects the ligation-induced structural changes in Hb that are involved in subunit communication.

Median Ligand Concentrations. Values for overall binding were determined by analysis for median ligand concentrations of the binding isotherms. The median value X_{med} of each O_2 binding isotherm, measured at Hb concentration P_t, was determined by numerical integration according to the Wyman relationship (*26*, *27*):

$$\int_0^{X_{med}} \overline{Y}\, dx = \int_{X_{med}}^{\infty} (1 - \overline{Y})\, dx \qquad (3)$$

Lower endpoints of the isotherms were well-determined, due to the relatively low affinity of these symmetric hybrids. The Fe^{2+} hemesites are only 85−95% saturated at atmospheric pressures of pure O_2; thus, to extrapolate the measured curves out to full saturation, a general three-parameter function of the form

$$y = \frac{a}{1 + \exp(-(x - x_0)/b)} \qquad (4)$$

was used to provide a smooth curve approximating the shape of the final portion of each isotherm. This general sigmoid function was fit to the uppermost 15% of each measured curve, along with a single point set at an $[O_2]$ of 10 mM, corresponding to 0.999 fractional saturation. To evaluate sensitivity of the integration procedure to the initial normalization parameters, 5% random error was applied to initial endpoint estimates and the extrapolation/integration sequence repeated, in a Monte Carlo fashion, over 1000 iterations. Error bars of the resulting X_{med} values then reflect the distributions of X_{med} values obtained by this procedure.

Overall Binding Constant Determination. The thermodynamic relationship between X_{med} and total protein concentration P_t has been derived (*25*) in terms of the equilibrium constants of deoxy and fully oxygenated species, i.e., for the linkage between dimer assembly and O_2 binding at the four stoichiometries of native HbA_0 ligation. Equations 5−7 comprise the corresponding relationships for the two-site binding case, applicable to species ***23***. The measured X_{med} vs P_t values were thus fit using eq 5,

$$X_{med} = \sqrt{\frac{(1 - {}^2f_2)}{K_{23}(1 - {}^0f_2)} \exp({}^0f_2 - {}^2f_2)} \qquad (5)$$

where

$${}^0f_2 = \frac{\sqrt{1 + 4({}^{01}K_2P_t)} - 1}{2({}^{01}K_2P_t)} \qquad (6)$$

and

$${}^2f_2 = \frac{\sqrt{1 + 4({}^{23}K_2P_t)} - 1}{2({}^{23}K_2P_t)} \qquad (7)$$

are the fractions of dimeric species corresponding respectively to the presence of zero and infinite ligand concentrations, $^{01}K_2$ is the equilibrium constant for dimer−tetramer assembly in the absence of ligand, and $^{23}K_2$ is the equilibrium constant when all Fe^{2+} hemes are ligated. Corresponding parameters for species ***24*** are K_{24} and $^{24}K_2$, respectively. From nonlinear regression analysis of these microstate systems, the respective best fit values for the overall tetrameric binding constants K_{23} and K_{24} were found by constraining $^{01}K_2$ and $^{23}K_2$ to their independently measured values and, alternatively, by constraining $^{01}K_2$ while allowing $^{23}K_2$ to vary.

Monte Carlo Error Analysis. Parameter resolvability was evaluated for the two-site linkage systems by employing a general Monte Carlo method to simulate O_2 data sets according to the fitting equations which describe ligand-linked dimer to tetramer equilibria for species ***23*** and ***24*** (Supporting Information). Parameter values used to generate

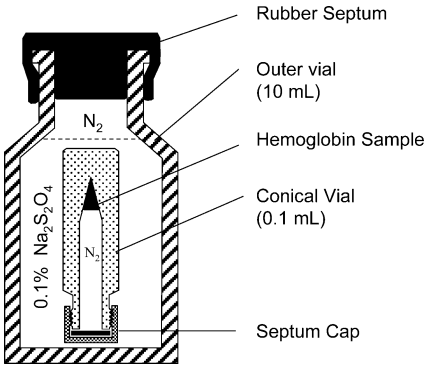

FIGURE 4: Long-term anaerobic incubation is conducted in a vial within a vial, in which the inner vial containing the sample is submerged in a solution of dithionite. The dithionite solution is prepared and the vials are assembled in an anaerobic chamber. The vial assembly is removed from the chamber and placed in a water bath set to the desired equilibration temperature. The outer vial is continuously purged with nitrogen or argon through needles inserted in the outer septum.

these curves represented the best-fit obtained from the experimental data, and the ranges and spacings of concentrations of Hb and O_2 were identical to those of the actual measured data sets. Pseudorandom noise was superimposed on the simulated data (*28*) using the subroutine RANNI from the Scientific Subroutine Library (SSR II, Lahey Fortran compiler) that generates pseudorandom numbers in accord with the normal distribution:

$$g(x) = \frac{1}{\sqrt{2\pi\sigma}} \exp\left[\frac{-(x-m)^2}{2\pi}\right] \qquad (8)$$

Using a mean value, $m = 0$, and standard deviation σ corresponding to 2−10% of the total range of fractional saturation, pseudorandom values were added to the simulated fractional saturation values at each O_2 concentration, and the perturbed data were subsequently fit with NONLIN. Distributions of the fitted parameters were generated from 1000 iterations of this process. Histograms were created using bin spacing of 0.05 kcal/mol over the range of best-estimate parameters. Errors presented here for parameters of each linkage system denote ±1 standard deviation of the resultant Monte Carlo distribution, corresponding to 3% random error in fractional saturation.

*Asymmetrically Ligated Hybrid Species **21***

Upon mixing Zn Hb with native Fe-heme deoxy Hb, the hybrid Zn/Fe species ***21u*** (species ***21*** unligated) tetramer is formed via a net dimer exchange among the parent species. Since both parents and hybrid have essentially the same assembly free energy when unligated, mixing the parent tetramers in a 1:1 ratio results in ∼50% hybrid tetramer at equilibrium, which is attained after ∼3 days (*10*). In the present study, the hybridization was carried out by first deoxygenating solutions of the parent ZnHb and FeHb species for 1 h in septum-sealed vials with continuous flushing under N_2. Equimolar amounts (0.5 mM each) of unligated parent species were mixed (using Hamilton gastight syringes) in a septum-sealed vial, which was then submerged in a larger vial containing 0.1% dithionite (Figure 4). These manipulations were carried out in a vinyl anaerobic chamber (Coy Laboratory Products, Inc.) at room temperature. The sealed vial was transferred out of the anaerobic chamber for incubation at 21.5 °C, during which the larger septum-sealed vial was purged with purified N_2.

Tetramer k_{off} from Dimer Trapping with Haptoglobin

Dissociation of Zn/FeO_2 tetramer species ***21*** and ***24*** to their constituent $\alpha\beta$ dimers was monitored in an Applied Photo-Physics SX.18MV stopped flow spectrophotometer which was cooled by an external water bath to 21.5 °C with a path length of 2 mm and dead time of 1 ms. The anaerobic mixture containing asymmetric hybrid species ***21u*** (unligated) along with symmetric parent species ***01*** (ZnHb) and ***41*** (native deoxyFeHb) was incubated for at least 24 h as described above. The anaerobic mixture was then added to deoxygenated standard buffer to a final concentration of 16 μM, followed by an anaerobic transfer to one of the drive syringes of the stopped flow spectrophotometer in a custom polymer anaerobic chamber (Coy Laboratory Products, Inc.) that had been continuously flushed with nitrogen for at least 48 h. A sample of haptoglobin (8 μM) previously equilibrated with either air, 100% O_2, or 100% CO was transferred to the other drive syringe of the stopped flow instrument. The absorbance change upon mixing was monitored for 500 s.

In the case of a hybrid mixture such as that for species ***21***, both parent tetramers (i.e., ZnHb species ***01*** and native oxyHb species ***41***) will also dissociate into dimers that react irreversibly with haptoglobin. For Zn/FeO_2 species ***21***, the maximum fraction of hybrid formed at equilibrium is only 3% of the mixture, as measured by sub-zero isoelectric focusing (*4*). However, under anaerobic conditions, the unligated species ***21u*** tetramer comprises nearly 30% of the hybrid mixture after 24 h of equilibration. Addition of O_2 to this anaerobic mixture results in rapid formation of species ***21***, followed by tetrameric dissociation and disproportionation to the parent species (Figure 5). The species ***21*** fraction of the hybrid mixture falls from 30% to 3% within a few seconds, and haptoglobin traps the free $\alpha\beta$ dimers as the tetramers dissociate. There is an accompanying change in absorbance for species ***21*** and ***01***, but no significant change in absorbance for species ***41***. The overall rate-limiting step of the observable process is dissociation of the species ***21*** tetramer, with the rate constant $^{21}k_{off}$.

The Zn/FeO_2 species ***24***, in which the α-subunits are ligated, can be studied in pure form rather than as a hybrid mixture. A 16 μM solution was equilibrated under flowing gas (either air, O_2, or CO) and reacted with haptoglobin in the stopped-flow as described above.

In all haptoglobin experiments, the absorbance decay followed a single exponential, which was fit either with TableCurve or SigmaPlot (Systat Software). Data are presented as averages of at least triplicates with standard deviations. Tetramer to dimer dissociation rate constants were combined with the consensus dimer to tetramer association rate constant ($k_{on} = 1.1 \times 10^6$ M^{-1} s^{-1}, independent of the presence or absence of bound ligand) to calculate assembly free energies ($\Delta G_2 = -RT \ln(k_{on}/k_{off})$) (*29*).

Construction of a Binding Isotherm from Microstate Constants

The free energies $^{ij}\Delta G_c$, ΔG_{ij} , and ΔG_{int} each have their logarithmic counterparts, which comprise the microstate

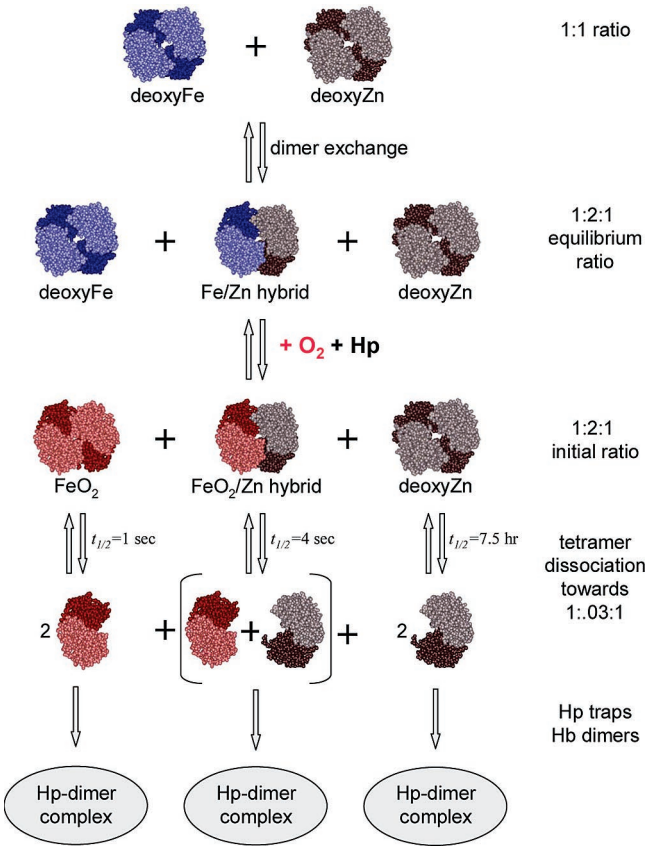

FIGURE 5: Reaction scheme for the formation and decay of Zn/Fe species ***21***. At the top of the scheme, native deoxyFeHb (blue) and ZnHb (brown) are mixed in a 1:1 molar ratio under anaerobic conditions. Dimer exchange between the two parent tetramers produces the unligated hybrid species ***21u*** over a time course of many hours ($t_{1/2}$ for dissociation of the deoxy tetramer to free dimer = 7.5 h). The anaerobic hybrid mixture is then mixed with a solution of haptoglobin (Hp) in the presence of O_2 or CO in the stopped-flow instrument. Species ***21*** is formed quickly from species ***21u*** (ligated hemes are denoted by red subunits). The three tetramers begin dissociating to form an equilibrium mixture in which the ***21*** hybrid comprises ~3% of the hybrid mixture. As the tetramers dissociate, the free dimers are trapped by haptoglobin in an essentially irreversible reaction. Formation of a complex between the deoxy free dimer and haptoglobin occurs with a decrease in absorbance, which reflects the rate-limiting step, i.e., dissociation of species ***21***. The reactions of the parent species with ligand and with haptoglobin do not contribute significantly to the absorbance signal (see text).

partition function, a model-independent function of all possible ligand binding constants,

$$\mathbf{Z} = 1 + (2k_{11} + 2k_{12})[O_2] + (2k_{21} + 2k_{22} + k_{23} + k_{24})[O_2]^2 + (2k_{31} + 2k_{32})[O_2]^3 + k_{41}[O_2]^4 \quad (9)$$

where the k_{ij} values are the microstate binding constants for each *ij* binding configuration multiplied by their individual statistical factors (*1*). Each k_{ij} constant is composed of an intrinsic binding constant k_{int} and a cooperativity term ${}^{ij}k_c$. Expanding the k_{ij} terms, the microstate partition function becomes

$$\mathbf{Z} = 1 + ({}^{11}k_c + {}^{12}k_c)(k_{int}[O_2]) + ({}^{21}k_c + {}^{22}k_c + {}^{23}k_c + {}^{24}k_c)(k_{int}[O_2])^2 + ({}^{31}k_c + {}^{32}k_c)(k_{int}[O_2])^3 + {}^{41}k_c(k_{int}[O_2])^4 \quad (10)$$

Here, **Z** is completely general in nature, accommodating any combination of values for each of the ${}^{ij}k_c$ constants.

*Calculation of Tetrameric Binding Isotherms for Species **21**, **23**, and **24***

Binding curves were constructed from experimentally determined tetrameric binding constants using the following equations for fractional saturation of hemesites. For species ***23***,

$$\overline{Y}_{23} = \frac{2k_{11}[O_2] + 2k_{23}[O_2]^2}{2(1 + 2k_{11}[O_2] + k_{23}[O_2]^2)} \quad (11)$$

where k_{11} is the constant for binding one ligand to an α-subunit (to make species ***11***) and k_{23} is the constant for binding two ligands, one to each α-subunit, to make species ***23***. The constant k_{11} is multiplied by a statistical factor of 2 since two identical binding sites (both α-subunits within the tetramer) are available for binding. The same equation holds for species ***24***, using k_{12} (binding one ligand to a β-subunit) and k_{24}, respectively. For species ***21***, fractional saturation reflects available binding sites on one α-subunit and one β-subunit:

$$\overline{Y}_{21} = \frac{(k_{11} + k_{12})[O_2] + 2k_{21}[O_2]^2}{2(1 + (k_{11} + k_{12})[O_2] + k_{21}[O_2]^2)} \quad (12)$$

The statistical factors for k_{11} and k_{12} are set to unity, as only one α- and one β-hemesite are available for binding in species ***21***.

These equations describe the binding isotherms when only tetramer species are present, generating tetrameric isotherms that are useful for comparative purposes, but are not truly representative of the experimentally observed isotherms (obtained with dilute solutions) in that the contribution of free dimers is not included.

RESULTS

*Noncooperative Isotherms for Species **23** and **24***

Oxygen binding isotherms were measured over a 4000-fold range of concentration of species ***23*** ($\alpha[Fe^{2+}O_2]$ $\beta[Zn^{2+}]$) and a 10000-fold range of concentration of species ***24*** ($\alpha[Zn^{2+}]$ $\beta[Fe^{2+}O_2]$) at pH 7.4 and 21.5 °C. The isotherms for each species exhibit a rightward shift with increasing protein concentration (Figure 6), corresponding to the increasing fractional abundance of tetramers relative to free dimers. In general, dissociation of the tetramer to its constituent free dimers increases upon both ligation and dilution. Both assembly and ligation processes must therefore be considered in order to analyze for purely tetrameric binding constants (*30*, *31*). To carry this out, the linked dimer−tetramer equilibria were incorporated into all data analyses of dilute Hb samples (*25*, *28*).

Visual inspection of the hyperbolic shape of the isotherms and the linear Hill transforms (shown as insets in Figure 6) indicated essentially noncooperative binding in these two-site species. The tendency toward positive cooperativity, evident at low protein concentration, is only an apparent effect arising from the significant concentrations of free dimers, which have high O_2 affinity. An overall low affinity

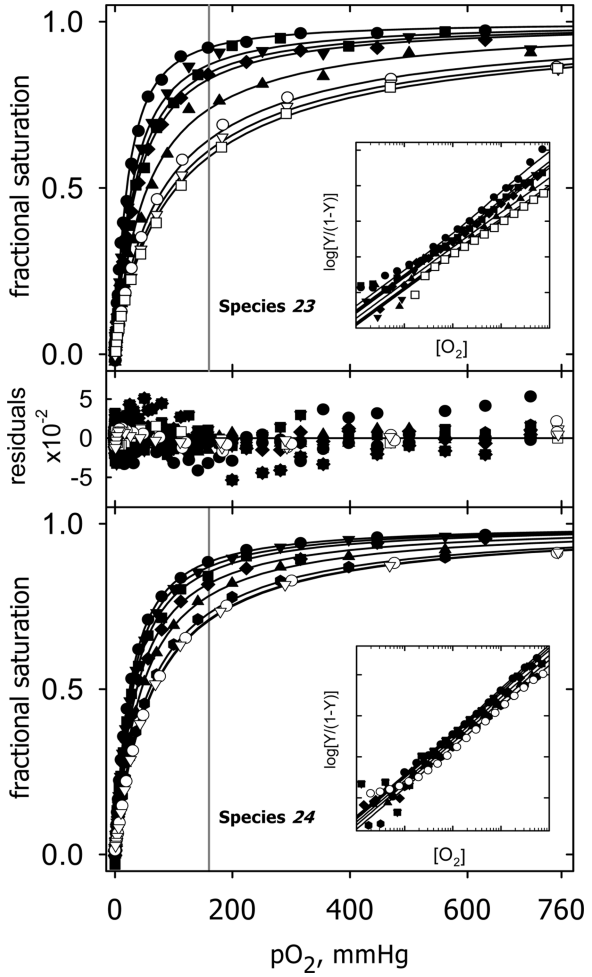

FIGURE 6: Oxygenation isotherms for Zn/Fe species ***23*** and ***24*** measured at a series of Hb concentrations under standard conditions of pH 7.4 and 21.5 °C using pure oxygen. A subset of data points from Imai cell experiments (filled symbols) and Gill cell experiments (open symbols) are plotted along with the global least-squares fits (lines) for both species. Residuals from the fit are shown in the center panel. The Hill transforms of representative fitted isotherms are given in the insets. The partial pressure of O_2 in air is 160 mmHg, indicated by the vertical gray line. (Upper panel) Isotherms measured for species ***23*** at concentrations of 0.3 μM (●), 0.7 μM (▼), 1.0 μM (■), 1.3 μM (◆), 4.2 μM (▲), 0.02 mM (○), 0.2 mM (▽), and 1.3 mM (□). (Lower panel) Isotherms measured for species ***24*** at concentrations of 0.3 μM (●), 0.6 μM (▼), 1.1 μM (■), 2.3 μM (◆), 6.2 μM (▲), and 69 μM (⬢), 1.0 mM (○), and 3.0 mM (▽).

of the tetramer for O_2 is indicated by the incomplete saturation at high concentrations of O_2 (i.e., 1 atm or 760 mmHg). Under atmospheric conditions (21% O_2), indicated by the vertical gray line, the doubly ligated species make up the majority of the Hb tetramers, but significant amounts of singly ligated species are present as well.

Global least-squares fitting of all isotherms for each species was carried out by constraining the deoxy assembly free energy to an independently measured value ($^{01}\Delta G_2 = -14.35 \pm 0.15$ kcal/mol (*10*) for each Zn-substituted species under these conditions). The absence of significant cooperativity (favorable or unfavorable) is evident in the best fit parameter values (Table 1). The intrinsic binding free energies, ΔG_{int}, for Zn-substituted free dimers exhibited a barely observable perturbation of 0.2 kcal/mol from those of native HbA_0. This difference falls close to the limits of error for these measurements, representing an increase in affinity that is negligible.

Table 1: O_2 Binding and Dimer−Tetramer Assembly Free Energies for Species ***23*** and ***24*** and Constituent Dimers (kcal/mol)

	Zn/FeO_2 Hb[a]	native Fe/FeO_2 Hb[b]
	Dimer Binding	
$^{\alpha}\Delta G_{int}$	-8.5 ± 0.1	-8.4 ± 0.1
$^{\beta}\Delta G_{int}$	-8.5 ± 0.1	-8.4 ± 0.1
$^{\alpha\beta}\Delta G_{int}$	-17.0 ± 0.1	-16.7 ± 0.1
	Tetramer Binding	
$\Delta G_{01\rightarrow11}$	-5.1 ± 0.1	-5.3 ± 0.1
$\Delta G_{11\rightarrow23}$	-4.9 ± 0.2	
$\Delta G_{01\rightarrow23}$	-10.0 ± 0.2	
$\Delta G_{01\rightarrow12}$	-5.3 ± 0.1	-5.3 ± 0.1
$\Delta G_{12\rightarrow24}$	-5.3 ± 0.1	
$\Delta G_{01\rightarrow24}$	-10.6 ± 0.1	
	Dimer−Tetramer Assembly	
$^{11}\Delta G_2$	-11.0 ± 0.1	-11.4 ± 0.3
$^{23}\Delta G_2$	-7.4 ± 0.2	
$^{12}\Delta G_2$	-11.2 ± 0.1	-11.4 ± 0.3
$^{24}\Delta G_2$	-8.0 ± 0.1	

[a] Determined in this study under standard conditions of 0.1 M Tris-HCl, 0.1 M NaCl (0.18 M total chloride), 1 mM Na_2EDTA, pH 7.4, 21.5 °C. [b] Average values from several independent resolutions of the linkage scheme (*26*, *32*, *33*).

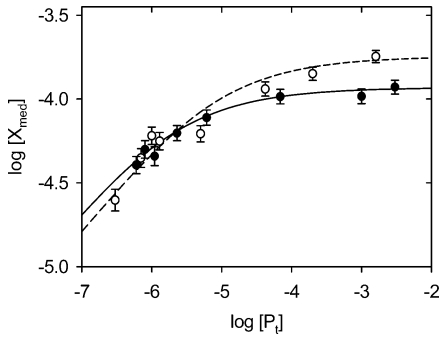

FIGURE 7: Logarithm of the median O_2 activity, X_{med}, for oxygenation to form Zn/Fe species ***23*** (open symbols) and ***24*** (filled symbols), calculated from the oxygenation isotherms as a function of molar Hb concentration P_t. Curves through the data (solid line for species ***23*** and dashed line for species ***24***) represent the best least-squares fit to eqs 5−7. Error bars on the data points represent one standard deviation of the distributions of X_{med} values after 1000 iterations using 5% random error applied to upper normalization end points of the isotherms before calculation.

Overall binding constants for the fully oxygenated tetramers were confirmed by analysis of the median ligand concentrations X_{med} (*34*), which is a fundamental parameter of each binding isotherm (*25*, *27*) that reflects the molar free energy for reacting all binding sites of the system. Median analysis relies on the same binding isotherms used in the global fit for Adair constants, but is not sensitive to detailed isotherm shape, thus providing the most rigorous determination of overall binding affinities and linked assembly free energies. The relationship between X_{med} and P_t for species ***23*** and ***24*** yielded overall binding constants in close agreement with results of the global linkage analysis (Figure 7). The least-squares fits of eqs 5−7 were obtained separately for species ***23*** and ***24*** by constraining $^{01}\Delta G_2$ to -14.35 ± 0.1 kcal/mol and allowing the remaining independent parameters to vary. Resolved overall binding free energies of the fully oxygenated tetramers were $\Delta G_{23} = -10.0 \pm 0.2$ and $\Delta G_{24} = -10.6 \pm 0.3$ kcal/mol, while assembly free energies were $^{23}\Delta G_2 = -7.1 \pm 0.3$ and $^{24}\Delta G_2 = -8.0 \pm 0.2$ kcal/mol. Further confirmation of these parameter values

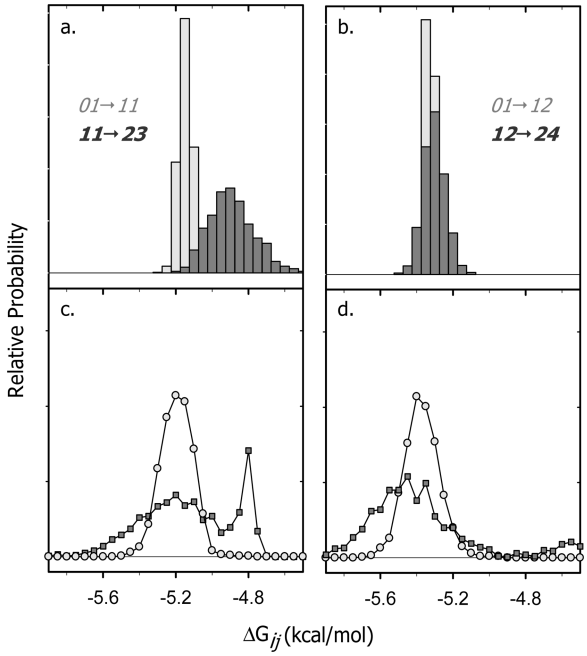

FIGURE 8: Probability distributions for the first and second stepwise binding free energies, ΔG_{ij}, for binding to form species ***23*** and ***24*** from data sets simulated with 3% random error. (a) The first ligand binding step ($\Delta G_{01\rightarrow11}$, light gray) and the second step ($\Delta G_{11\rightarrow23}$, dark gray). (b) The first binding step ($\Delta G_{01\rightarrow12}$, light gray) and the second step ($\Delta G_{12\rightarrow24}$, dark gray). In both analyses shown in panels a and b the synthetic data was generated over a range of Hb concentrations similar to that shown in Figure 6. Analyses based on synthetic data from a single Hb concentration are shown in (c) the first binding step ($\Delta G_{01\rightarrow11}$, light gray circles) and the second step ($\Delta G_{11\rightarrow23}$, dark gray boxes) and (d) the first binding step ($\Delta G_{01\rightarrow12}$, light gray circles) and the second step ($\Delta G_{12\rightarrow24}$, dark gray boxes).

was provided by their close agreement with previous determinations of the assembly free energies for these ligated hybrid species using analytical gel chromatography methods (*10*)

Resolvability of the first and second stepwise binding constants was analyzed by a general Monte Carlo analysis of synthetic data sets generated with the experimentally determined tetrameric binding constants (Figure 8). Improvement in resolvability through the use of concentration-dependent synthetic data sets is observed in the case of binding to form species ***23***, in which a slight difference in binding constants is measured.

*Positive Cooperativity in Species **21***

Tetramer to dimer dissociation rate constants were determined by mixing Hb with human haptoglobin (*10*, *29*, *35*), which is a dimeric protein capable of irreversibly binding two Hb dimers. The rate of the overall reaction is limited by the rate of Hb tetramer dissociation. The absorbance decrease in the Soret region that accompanies the formation of the haptoglobin−deoxy dimer complex has provided a very useful tool for determining dimer → tetramer assembly constants, $^{ij}\Delta G_2$, for both modified and native Hbs over a range of solution conditions (*29*, *32*, *36*−*38*). The reaction of haptoglobin with fully ligated species ***41*** is rapid ($t_{1/2}$ = 1 s), but does not result in an appreciable change in absorbance. Reaction of haptoglobin with the parent species ***01*** and the hybrid ***21*** does produce a change in absorbance

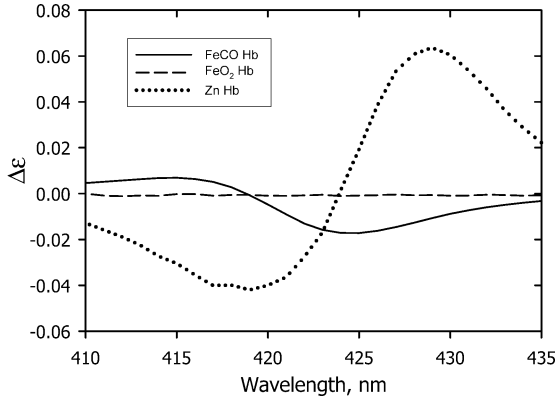

FIGURE 9: Comparison of absorbance change upon reaction with the free dimers of Hb and human haptoglobin between oxy and carbon monoxy dimers and the deoxy dimer, shown here with Zn Hb, the relevant deoxy species in the reaction of Figure 10.

(Figure 9). The reaction with species ***01*** follows a very slow dissociation rate ($t_{1/2}$ = 7.5 h) (*35*), which does not contribute significantly to the kinetic profile.

The decrease in absorbance for the hybrid mixture was readily fit to a single exponential with a rate constant of 0.20 ± 0.02 s^{-1} (Figure 10, upper panel). The rate constant had the same value in the presence of 21% O_2 (air), 100% O_2 (1 atm of O_2), and was not significantly different in the presence of CO (0.18 ± 0.05 s^{-1}). When combined with the dimer → tetramer k_{on} value of 1.1 × 10^6 M^{-1} s^{-1} (*29*), these results yielded a value of $^{21}\Delta G_2$ of −9.1 ± 0.1 kcal/mol for Zn/FeO_2 and −9.2 ± 0.1 kcal/mol for Zn/FeCO. The value for k_{on} was previously determined with deoxy species ***01*** and has been shown to be invariant among a wide range of modifications and mutations to the tetramer (*29*). The insensitivity of $^{21}k_{off}$ to ligand concentration observed here indicates that partial ligation of this species is not significant, i.e., that the abundance of species ***11*** and ***12*** is very low and does not affect the evaluation of species ***21***.

Assignment of the observed absorbance change to dissociation of the hybrid tetramer, and not a parent tetramer, was addressed by the following controls. The ZnHb parent tetramer was incubated under the same anaerobic conditions used to incubate the hybrid mixture, and then reacted with an oxygenated solution of haptoglobin, resulting in only very small perturbations in absorbance over a 20 s period. This procedure was repeated with the FeHb parent, and a small absorbance change of ∼0.01 au was observed during the first 200 ms, attributable to oxygenation of the unligated Hb mixture. Alternatively, the separately incubated parents were combined immediately prior to loading them into the drive syringe of the stopped flow instrument. In this case, only a very small amount of hybrid species ***21u*** would be formed prior to mixing with haptoglobin, and the resulting reaction yielded a small signal change (Figure 10, upper panel, 0.5 h). In another control experiment, the anaerobic hybrid mixture was reacted with an oxygenated buffer solution which contained no haptoglobin, resulting in a small absorbance change due to oxygenation, as observed in the FeHb parent control. The dependence of amplitude on incubation time observed in these studies was compared to the time course for species ***21u*** formation that was previously measured by sub-zero isoelectric focusing (*4*), simulated from the observed assembly rate constants of both parents and

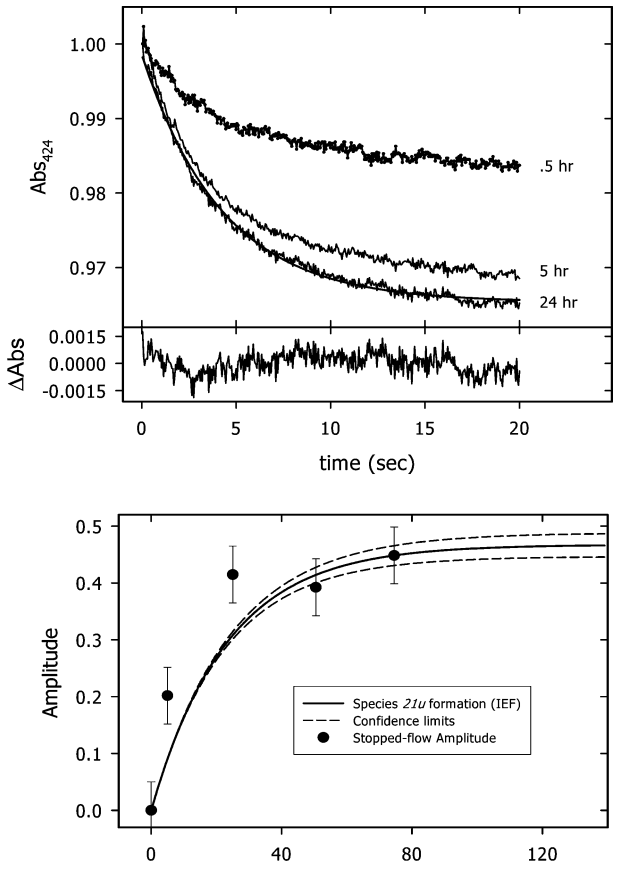

FIGURE 10: Reaction of an oxygenated solution of haptoglobin with the species ***21u*** hybrid mixture. (Upper panel) Representative stopped-flow traces for reaction after 0.5, 5, and 24 h of anaerobic incubation. The reaction time course after 24 h of incubation is fit with a single exponential, whose residual is shown below the panel. Concentrations are a total of 8 μM Fe^{2+} heme-containing subunits, 8 μM Zn^{2+} heme-containing subunits, and 8 μM haptoglobin. (Lower panel) Comparison of the time dependence of amplitudes of the reactions illustrated in the top panel with the time course of formation of the anaerobic species ***21u*** measured in equilibrium studies using cryogenic isoelectric focusing, plus confidence limits (*4*). The amplitudes measured by stopped-flow are normalized to the maximum fraction of hybrid from the isoelectric focusing study in order to permit comparison of time dependencies. Errors for the kinetic amplitudes are ±10% of the total change in amplitude. The zero point amplitude results from subtraction of control experiments.

hybrid (*4*). The increase in amplitude with incubation time is consistent with the formation of species ***21u*** (Figure 10, lower panel).

The results from this analysis yielded an assembly free energy for the Zn/FeO_2 species ***21*** tetramer that agrees well with the previously reported value for this species at equilibrium (*4*), and also demonstrates that partial ligation of the Fe-hemesites, if present, is too small to appreciably affect this result. The haptoglobin reaction with Zn/FeO_2 species ***24***, which was also carried out, exhibited a marked difference in assembly free energy between the Zn/FeO_2 tetramer (-8.7 ± 0.1 kcal/mol when equilibrated with 100% O_2) and the Zn/FeCO tetramer (-8.2 ± 0.1 kcal/mol), consistent with the O_2 binding results that showed incomplete ligation in species ***23*** and ***24*** even at 1 atm of O_2. The more negative assembly free energy in the oxygenated species ***24*** is consistent with the presence of singly oxygenated species ***12***, which has an assembly free energy that is more negative than that of species ***24***, resulting in a more negative apparent $^{24}\Delta G_2$.

Cooperative Free Energies of Hemesite Binding

To assess the relevance of the microstate measurements reported here for species ***21***, ***23***, and ***24*** to the rest of the Hb cascade, the experimentally determined binding and assembly constants are converted to cooperative free energy values. Cooperative free energy for each of the *ij* microstates, $^{ij}\Delta G_c$, is defined for each doubly ligated (2*j*) microstate as the change in the assembly free energy upon ligation:

$$^{2j}\Delta G_c = {}^{2j}\Delta G_2 - {}^{01}\Delta G_2 \qquad (13)$$

$^{ij}\Delta G_c$ is directly related to the ligand binding free energy, ΔG_{ij} , by the following linkage relations (Figure 3):

$$^{2j}\Delta G_c = \Delta G_{2j} - 2\Delta G_{int}$$
$$k_{2j} = k_{int}k_c \qquad (14)$$

where ΔG_{int} is the (intrinsic) free energy of binding to the free $\alpha\beta$ dimer. By thermodynamic linkage, the change in the assembly free energy upon ligation is equal to the change in ligation free energy upon assembly.

The cooperative free energy values for species ***23*** and ***24*** determined in the present study are very similar to those previously determined by large-zone chromatography and low-temperture isoelectric focusing (Table 2) (*10*). The values that have been significantly altered are those for the first binding step, i.e., for Zn/FeO_2 species ***11*** and ***12***, which are now more positive. The cooperative free energy value for species ***21*** is unchanged in comparison with that measured with sub-zero isoelectric focusing.

DISCUSSION

Analysis of partially ligated Hb microstates from this laboratory over the past decade has revealed an asymmetric distribution of cooperativity among the tetramers that comprise the binding cascade. The Hb tetramer is a dimer of $\alpha\beta$ dimers, exhibiting intradimer cooperativity as well as cooperativity between the two dimers (cross-dimer cooperativity). The presence of two levels of communication within the tetramer is particularly evident in the second binding step: Hb with two ligands bound to one dimer is thermodynamically more stable than Hb with one ligand on each dimer.

The populations of the eight structurally unique intermediates, or microstates, generated during ligand binding are greatly suppressed relative to the two end-states (i.e., the deoxy and fully ligated tetramers) as a consequence of positive cooperativity. Further complicating their experimental characterization, the microstates are in constant exchange with one another, via exchange of $\alpha\beta$ dimers among tetramers as well as exchange of the labile O_2 ligand among hemesites. Through the use of nonlabile hemesite analogs, the intermediate binding constants for each step in the binding cascade were determined by means of thermodynamic linkage between dimer → tetramer assembly and tetramer ligation affinity.

In the present investigation, employing the Zn-substituted analog for deoxy hemesites, it is demonstrated that binding

Table 2: Free Energies for Binding Oxygen by Hb Microstates (kcal/mol)

species	source	ΔG_2	ΔG_c	$\Delta G_{binding}$	$K_{binding}$
01	consensus[a]	-14.4 ± 0.1			
	Zn/FeO_2[b]	-14.3 ± 0.2			
11	consensus	-11.5	2.9	-5.5	1.1×10^4
	Zn/FeO_2	-11.4 ± 0.2	2.9 ± 0.3	-5.5 ± 0.3	$1.1 \pm 0.7 \times 10^4$
	this study	-11.0 ± 0.1	3.4 ± 0.1	-5.1 ± 0.1	$0.6 \pm 0.1 \times 10^4$
12	consensus	-11.5	2.9	-5.5	1.1×10^4
	Zn/FeO_2	-11.4 ± 0.2	2.9 ± 0.3	-5.5 ± 0.3	$1.1 \pm 0.7 \times 10^4$
	this study	-11.2 ± 0.1	3.1 ± 0.1	-5.3 ± 0.1	$0.9 \pm 0.1 \times 10^4$
21	consensus	-9.2	5.2	-11.5	3.4×10^8
	Zn/FeO_2	-9.2 ± 0.2	5.1 ± 0.3	-11.6 ± 0.3	$4.0 \pm 3 \times 10^8$
	this study	-9.1 ± 0.1	5.2 ± 0.1	-11.8 ± 0.2	$5.7 \pm 2 \times 10^8$
22	consensus	-7.2	7.2	-9.5	1.1×10^7
	Zn/FeO_2	-7.7 ± 0.3	6.6 ± 0.4	-10.1 ± 0.4	$3.1 \pm 3 \times 10^7$
23	consensus	-7.2	7.2	-9.5	1.1×10^7
	Zn/FeO_2	-7.5 ± 0.2	6.8 ± 0.3	-9.9 ± 0.3	$2.2 \pm 2 \times 10^7$
	this study	-7.4 ± 0.2	6.9 ± 0.2	-10.0 ± 0.2	$2.6 \pm 9 \times 10^7$
24	consensus	-7.2	7.2	-9.5	1.1×10^7
	Zn/FeO_2	-7.8 ± 0.2	6.5 ± 0.3	-10.2 ± 0.3	$3.7 \pm 2 \times 10^7$
	this study	-8.0 ± 0.1	6.3 ± 0.1	-10.6 ± 0.1	$7.3 \pm 1 \times 10^7$
31	consensus	-7.2	7.2	-17.9	1.7×10^{13}
	Zn/FeO_2	-7.4 ± 0.2	6.9 ± 0.3	-18.2 ± 0.3	$3.2 \pm 2 \times 10^{13}$
32	consensus	-7.2	7.2	-17.9	1.7×10^{13}
	Zn/FeO_2	-7.4 ± 0.2	6.9 ± 0.3	-18.2 ± 0.3	$3.2 \pm 2 \times 10^{13}$
41	consensus	-8.0 ± 0.1	6.4 ± 0.1	-27.0	1.1×10^{20}
	Fe/FeO_2[c]	-8.0 ± 0.1	6.3 ± 0.2	-27.1 ± 0.1	$1.3 \pm 0.3 \times 10^{20}$
free dimer (intrinsic)	1992[c]			-8.4	1.6×10^6
	2000[b]			-8.4 ± 0.1	$1.6 \pm 0.3 \times 10^6$
	this study[d]			-8.5 ± 0.1	$2.0 \pm 0.3 \times 10^6$

[a] Ackers et al. (*3*), "consensus" ΔG_2 values predicted from O_2 binding Adair constants. [b] Ackers et al. (*4*). [c] Chu et al. (*32*). [d] Intrinsic binding values when Zn heme is present in the dimer.

two ligands to the same dimer occurs with positive cooperativity, while binding one ligand to each dimer occurs with no favorable cooperativity, and is therefore a very low affinity binding process. Both types of ligand configuration contribute to the overall process of binding four O_2 ligands to Hb.

The First Binding Step in Hb Oxygenation Is Incomplete

In highly cooperative systems, it is intuitive that the first step in the process may not go to completion prior to the initiation of the second step. In the case of human Hb, the first binding step does not result in 100% of the tetramers containing a single ligand. Indeed, the first binding constant, K_1 (1×10^4 M^{-1} s^{-1} under conditions of this study, Table 2), predicts incomplete binding to Fe-hemesites in singly ligated Hb tetramers, or only ~75% occupancy of a single binding site per tetramer in air, as illustrated in Figure 11. The binding constants determined for the singly ligated Zn/FeO_2 microstate species ***11*** and ***12*** combine to give a macroscopic binding constant within error of the Adair K_1, which is measured with native Hb using traditional O_2 binding techniques (*10, 32*). It is interesting to note that the present conditions (low temperature, absence of organic phosphate) are actually "high affinity" conditions: at physiological conditions, the oxygen binding affinity is considerably decreased, and the first binding step will be even lower than observed here.

Complete, Cooperative Intradimer Binding at the Second Step

The demonstration of partial oxygenation in the singly ligated species ***11*** and ***12*** and in the doubly ligated species ***23*** and ***24*** raises the issue of partial oxygenation in species ***21***, in which both O_2 ligands are bound to the same dimer. The previously reported measurement of species ***21*** by sub-zero isoelectric focusing was conducted in a hybrid mixture with both parent tetramers, the fully Zn-substituted species ***01*** and the native Fe FeO_2 species ***41*** (*4*). Partial ligation of species ***21*** would have generated a mixture containing species ***11*** and ***12***, which may focus with the hybrid species ***21***. Thus, the extent of ligation of species ***21*** could not be ascertained from the isoelectric focusing result. In the present study, the rate constant for dissociation of the tetramer to free dimer was measured for species ***21*** in an experiment independent of the sub-zero isoelectric focusing experiment. These kinetic results confirmed the equilibrium results, yielding $^{21}\Delta G_c = 5.2 \pm 0.1$ kcal/mol, demonstrating that Zn/FeO_2 species ***21*** is fully ligated at equilibrium.

The use of nonlabile O_2 analogs and nonbinding deoxy hemesite analogs has served an important role in the deconvolution of Hb's binding curve into its microstate free energy components. The use of analogs always carries with it the caveat of artifact, but, to date, the distribution characteristics of cooperative free energy among the Hb microstates is independent of the type of analog used. One of the most critical aspects of these measurements lies in the analysis of experimental error. Techniques for studying the microstates have been developed with great attention to controlling uncertainty in the resolved values of microstate assembly free energy. This has been necessary, considering that the "energetic distance" between the two end-states, deoxy and oxy Hb, is 6.3 ± 0.1 kcal/mol at 21.5 °C, providing rather narrow limits within which eight additional species must be clearly defined. The difficulty in carrying this out in Hb has historically been reflected in the Adair

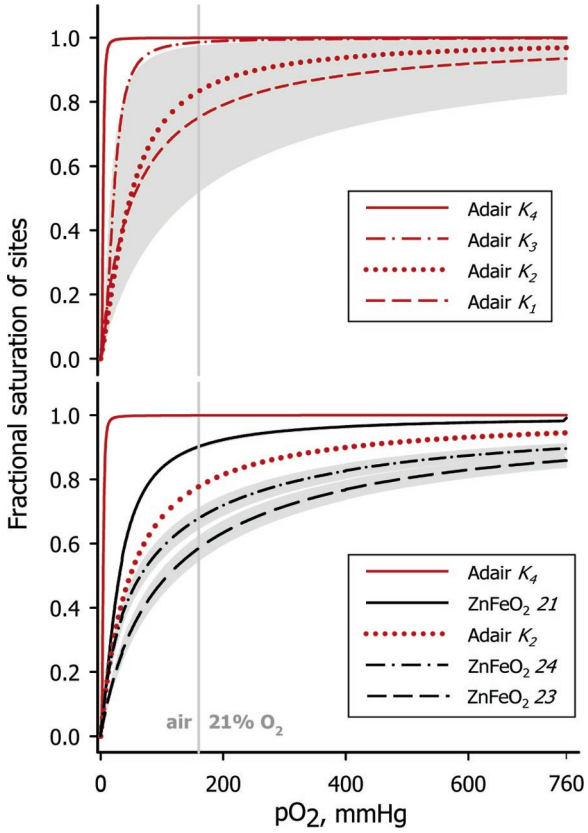

FIGURE 11: Comparison of calculated O_2 isotherms for native FeHb and ZnHb illustrating incomplete ligation for singly and doubly ligated species. The partial pressure of O_2 in air is 160 mmHg, indicated by the vertical gray line. (Upper panel) Binding curves calculated from each of the stoichiometric Adair constants measured by direct O_2 binding to native Hb. The error envelope for the second binding constant, K_2, is shown as the shaded area. The error for K_3 is similar in magnitude (not shown). The tetramer Adair constants were determined by global fitting to Hb concentration-dependent isotherms under the same conditions as those of the present study (*32*). (Lower panel) Isotherms from assembly constants for species ***21*** $ZnFeO_2$, species ***23*** $ZnFeO_2$, and species ***24*** $ZnFeO_2$ (black lines) (Table 2) are compared with Adair isotherms for binding two and four ligands (red lines).

constants, in which the goal is much simpler, with only two intermediate binding constants needed. Even so, the errors in K_2 and K_3 are sufficiently large that their best-fit ranges of uncertainty overlap (*1*, *32*).

Incomplete, Noncooperative Cross-Dimer Binding at the Second Step

If the first binding constant is extended to the second binding step, i.e., in noncooperative binding, a similar extent of (incomplete) ligation is expected. The present finding of noncooperative, incomplete binding to form the symmetrically ligated Zn/FeO_2 species ***23*** and ***24*** is consistent with this expectation. The present observation is also in agreement with predictions from the microstate *consensus distribution* of 1992 (which was based on the $Fe^{2+}/Fe^{3+}CN$, Fe^{2+}/Mn^{3+}, and $Co^{2+}/FeCO$ analog systems) and with subsequent O_2 binding measurements for Zn/FeO_2 species ***23*** and ***24*** from other laboratories (*12*, *39*). In native Hb, the macroscopic Adair constant K_2 is measured with a relatively high experimental error even under the most rigorous conditions (*26*, *32*, *33*). The macroscopic K_2 represents an average value of the composite: $2k_{21} + 2k_{22} + k_{23} + k_{24}$. Comparison with present results shows that binding to form Zn/FeO_2 species ***23*** and ***24*** is less cooperative than the Adair value, while binding to species ***21*** is more cooperative, and, in combination, the microstate constants yield a macroscopic binding constant that is in agreement with the Adair K_2.

A slight anticooperativity in binding to form ***22***, ***23***, and ***24*** may be present, but this is observed as a trend, not as a significant difference in absolute values of the binding constants. Apparent anticooperativity in these binding steps, observed in previously published data from this laboratory (*4*, *10*), as noted by Noble and colleagues (*12*), is enhanced by incomplete ligation of both singly ligated species, ***11*** and ***12***, and doubly ligated species ***22***, ***23***, and ***24***. When incomplete ligation is properly accounted for, as in the present study, the anticooperativity is replaced by noncooperativity. Still, the presence of a small degree of anticooperativity cannot be ruled out within experimental error. It should be noted that hemesite heterogeneity, such as differences in α- and β-subunit affinities, will also manifest as anticooperativity. Shibayama and co-workers reported oxygen binding to form the Zn/FeO_2 species ***23*** and ***24*** with a slight favorable cooperativity (*39*), while Noble and co-workers reported noncooperative binding (*12*). Although Shibayama and co-workers did not include an analysis of experimental error, the apparent cooperativity observed is likely due to the presence of free dimer (which has a high O_2 affinity) in the dilute solution used in those experiments, as suggested by Noble and co-workers (*12*).

Significant Differences and Error Propogation

The laboratories of Shibayama and Morimoto have reported that the ligand binding constant for species ***21*** Zn/FeO_2 is the same as that for the other doubly ligated species (*40*). These authors argue that their use of an O_2-jump stopped-flow experiment gives correct values for O_2 binding constants for species ***21*** ($^{21}\Delta G_c = 5.4$ kcal/mol) while the value of 5.1 ± 0.3 kcal/mol determined in this laboratory by sub-zero isoelectric focusing is incorrect. Their report of the O_2-jump experiment and the comparison of binding constants from the two laboratories was published in the absence of an analysis of experimental error. An estimate of experimental error may be drawn from these authors' conclusions that the binding constants for species ***21*** are "essentially identical" to those for species ***23*** and ***24*** measured by established equilibrium binding techniques in a previous report by the same laboratory (*39*). This error estimate is ±0.75 kcal/mol, placing the value for species ***21*** binding constants reported by this laboratory well within the apparent error envelope of the O_2-jump technique. The experimental error associated with the O_2-jump technique is of particular importance in the comparisons made by these authors, since the data consists of relatively few points over a very narrow range of O_2 concentration, and the parameter estimate was based on the extrapolation of a kinetic phase to zero time.

Are the Zn/FeO_2 Tetramers in the T State or the R State?

This and previous studies (*12*, *39*) have shown that O_2 binding to form species ***23*** and ***24*** occurs with the low affinity of the first binding constant, K_1, observed in

unmodified human Hb. It has been suggested that this low affinity binding is a result of the Zn^{2+}-heme substitution favoring the formation of T-state Hb, i.e., the structure and properties of deoxyHb (*39*). The T-state designation is a model commonly used to describe the O_2 binding affinity of deoxy Hb. Thus, O_2 binding to a T-tetramer is, by definition of the model, low affinity. If the Zn/FeO_2 species were indeed in the T state, then the binding of the third ligand to either of these species would also be low affinity. By contrast, however, the third stepwise binding free energies show a 120-fold increase, consistent with that of native Hb (Table 2, Figure 1). A wide range of functional and structural properties have been ascribed to both the T and R states of human Hb, consistent with models in which multiple states of both T and R are permitted (*12*, *41*). Given this demonstrated lack of specificity, it may seem that the simple concept of T and R has outlived its usefulness in providing an unambiguous, testable model for further characterization of cooperativity in Hb.

In summary, low affinity, incomplete ligation, and absence of cooperativity in these Zn/FeO_2 species are consistent with macroscopic binding properties of native Fe/FeO_2 Hb (the Adair constants K_1 and K_2), suggesting that the microscopic binding constants are not artifacts of Zn-substitution, which is addressed in the accompanying paper (*14*). *Zn-substituted heme appears to be, in fact, an excellent analog of deoxyFe heme, in that it is possible to observe the incomplete ligation in the first binding step that is predicted by the native Adair constant.*

SUPPORTING INFORMATION AVAILABLE

Derivation of the fitting functions for protein-concentration dependent binding isotherms. This material is available free of charge via the Internet at http://pubs.acs.org.

REFERENCES

1. Ackers, G. K. (1998) Deciphering the molecular code of hemoglobin cooperativity, *Adv. Protein Chem. 51*, 185−253.
2. Smith, F. R., and Ackers, G. K. (1985) Experimental resolution of cooperative free energies for the ten ligation states of human hemoglobin, *Proc. Natl. Acad. Sci. U.S.A. 82*, 5347−5351.
3. Ackers, G. K., Doyle, M. L., Myers, D., and Daugherty, M. A. (1992) Molecular code for cooperativity in hemoglobin, *Science 255*, 54−63.
4. Ackers, G. K., Holt, J. M., Huang, Y., Grinkova, Y., Klinger, A. L., and Denisov, I. (2000) Confirmation of a unique intradimer cooperativity in the human hemoglobin $\alpha^1\beta^1$ half-oxygenated intermediate supports the symmetry rule model of allosteric regulation, *Proteins: Struct., Funct., Genet. Suppl. 4*, 23−43.
5. Goldbeck, R. A., Esquerra, R. M., Holt, J. M., Ackers, G. K., and Kliger, D. S. (2004) The molecular code for hemoglobin allostery revealed by linking the thermodynamics and kinetics of quaternary structural change. 1. Microstate linear free energy relations, *Biochemistry 43*, 12048−12064.
6. Goldbeck, R. A., Esquerra, R. M., Kliger, D. S., Holt, J. M., and Ackers, G. K. (2004) The molecular code for hemoglobin allostery revealed by linking the thermodynamics and kinetics of quaternary structural change. 2. Cooperative free energies of $(\alpha FeCO\beta Fe)_2$ and $(\alpha Fe\beta FeCO)_2$ T-state tetramers, *Biochemistry 43*, 12065−12080.
7. Ackers, G. K., Dalessio, P. M., Lew, G. H., Daugherty, M. A., and Holt, J. M. (2002) Single Residue Modification of Only One Dimer within the Hemoglobin Tetramer Reveals Autonomous Dimer Function, *Proc. Natl. Acad. Sci. U.S.A. 99*, 9777−9782.
8. Silva, M. M., Rogers, P. H., and Arnone, A. (1992) A third quaternary structure of human hemoglobin A at 1.7 A resolution, *J. Biol. Chem. 267*, 17248−17256.
9. Kavanaugh, J. S., Rogers, P. H., Case, D. A., and Arnone, A. (1992) High-resolution x-ray study of deoxyhemoglobin Rothschild 37β Trp to Arg: a mutation that creates an intersubunit chloride-binding site, *Biochemistry 31*, 4111−4121.
10. Huang, Y., Doyle, M. L., and Ackers, G. K. (1996) The oxygen-binding intermediates of human hemoglobin: evaluation of their contributions to cooperativity using zinc-containing hybrids, *Biophys. J. 71*, 2094−2105.
11. Huang, Y., Yonetani, T., Tsuneshige, A., Hoffman, B. M., and Ackers, G. K. (1996) Heterometallic hybrids of homometallic human hemoglobins, *Proc. Natl. Acad. Sci. U.S.A. 93*, 4425−4430.
12. Samuni, U., Juszczak, L., Dantsker, D., Khan, I., Friedman, A. J., Pérez-González-de-Apodaca, J., Bruno, S., Hui, H. L., Colby, J. E., Karasik, E., Kwiatkowski, L. D., Mozzarelli, A., Noble, R., and Friedman, J. M. (2003) Functional and spectroscopic characterization of half-liganded iron−zinc hybrid hemoglobin: evidence for conformational plasticity within the T state, *Biochemistry 42*, 8272−8288.
13. Ackers, G. K., Holt, J. M., Burgie, E. S., and Yarian, C. S. (2004) Analyzing intermediate state cooperativity in hemoglobin, in *Methods in Enzymology* (Holt, J. M., Johnson, M. J., and Ackers, G. K., Ed.) pp 3−28, Elsevier, San Diego, CA.
14. Holt, J. M., and Ackers, G. K. (2005) Asymmetric distribution of cooperativity in the binding cascade of normal human hemoglobin. 2. Stepwise cooperative free energy, *Biochemistry 44*, XXXXX−XXXXX.
15. Naito, N. R., Huang, H., Sturgess, A. W., Nocek, J. M., and Hoffman, B. M. (1998) Binding and electron transfer between cytochrome b_5 and the hemoglobin α- and β-subunits through the use of [Zn, Fe] hybrids, *J. Am. Chem. Soc. 120*, 11256−11262.
16. Scholler, D. M., Wang, M. Y. R., and Hoffman, B. M. (1978) Metal-substituted hemoglobin and other hemoproteins, *Methods Enzymol. 52*, 487−493.
17. Grassetti, D. R., and Murray, J. F. (1967) Determination of sulfhydryl groups with 2,2′- or 4,4′-dithiopyridine, *Arch. Biochem. Biophys. 119*, 41−49.
18. Hoard, J. L. (1971) Stereochemistry of hemes and other metalloporphyrins, *Science 174*, 1295−1302.
19. Imai, K. (1981) Measurement of accurate oxygen equilibrium curves by an automatic oxygenation apparatus, *Methods Enzymol. 76*, 438−439.
20. Hayashi, A., Suzuki, T., and Shin, M. (1973) An enzymatic reduction system for metmyoglobin and methemoglobin, and its application to functiional studies of oxygen carriers, *Biochim. Biophys. Acta 310*, 309−316.
21. Dolman, D., and Gill, S. J. (1978) Membrane-covered thin-layer optical cell for gas reaction studies of hemoglobin, *Anal. Biochem. 87*, 127−134.
22. Kiger, L., Klinger, A. L., Kwiatkowski, L. D., DeYoung, A., Doyle, M. L., Holt, J. M., Noble, R. W., and Ackers, G. K. (1998) Thermodynamic studies on the equilibrium properties of a series of recombinant βW37 hemoglobin mutants, *Biochemistry 37*, 4336−4345.
23. Wilhelm, E., Battino, R., and Wilcock, R. J. (1977) Low-pressure solubility of gases in liquid water, *Chem. Rev. 77*, 219−262.
24. Johnson, M. L., and Frasier, G. S. (1985) Nonlinear least-squares analysis, *Methods Enzymol. 117*, 301−342.
25. Johnson, M. L., Halvorson, H. R., and Ackers, G. K. (1976) Oxygenation-linked subunit interactions in human hemoglobin: analysis of linkage functions for constituent energy terms, *Biochemistry 15*, 5363−5371.
26. Doyle, M. L., Holt, J. M., and Ackers, G. K. (1997) Effects of NaCl on the linkages between O_2 binding and subunit assembly in human hemoglobin: titration of the quaternary enhancement effect, *Biophys. Chem. 64*, 271−287.
27. Wyman, J. (1964) Linked functions and reciprocal effects in hemoglobin: a second look, *Adv. Protein Chem. 19*, 223−286.
28. Doyle, M. L., Myers, D. W., Ackers, G. K., and Shrager, R. I. (1994) Weighted nonlinear regression analysis of highly cooperative oxygen equilibrium curves, *Methods Enzymol. 232*, 576−597.
29. Turner, G. J., Galacteros, F., Doyle, M. L., Hedlund, B., Pettigrew, D. W., Turner, B. W., Smith, F. R., Moo-Penn, W., Rucknagel, D. L., and Ackers, G. K. (1992) Mutagenic dissection of hemoglobin cooperativity: effects of amino acid alteration on subunit assembly of oxy and deoxy tetramers, *Proteins: Struct., Funct., Genet. 14*, 333−350.

30. Ackers, G. K., and Halvorson, H. R. (1974) The linkage between oxygenation and subunit dissociation in human hemoglobin, *Proc. Natl. Acad. Sci. U.S.A. 71*, 4312−4316.
31. Klinger, A. L., and Ackers, G. K. (1998) Analysis of spectra from multiwavelength oxygen-binding studies of mixed metal hybrid hemoglobins, *Methods Enzymol. 295*, 190−207.
32. Chu, A. H., Turner, B. W., and Ackers, G. K. (1984) Effects of protons on the oxygenation-linked subunit assembly in human hemoglobin, *Biochemistry 23*, 604−617.
33. Mills, F. C., Johnson, M. L., and Ackers, G. K. (1976) Oxygenation-linked subunit interactions in human hemoglobin: experimental studies on the concentration dependence of oxygenation curves, *Biochemistry 15*, 5350−5362.
34. Wyman, J., and Gill, S. J. (1990) *Binding and Linkage. Functional Chemistry of Biological Macromolecules*, University Science Books, Mill Valley, CA.
35. Ip, S. H. C., Johnson, M. L., and Ackers, G. K. (1976) Kinetics of deoxyhemoglobin subunit dissociation determined by haptoglobin binding: estimation of the equilibrium constant from forward and reverse rates, *Biochemistry 15*, 654−660.
36. Huang, Y., and Ackers, G. K. (1995) Enthalpic and entropic components of cooperativity for the partially ligated intermediates of hemoglobin support a "Symmetry Rule" mechanism, *Biochemistry 34*, 6316−6327.
37. Huang, Y., and Ackers, G. K. (1996) Transformation of cooperative free energies between ligation systems of hemoglobin: resolution of the carbon monoxide binding intermediates, *Biochemistry 35*, 704−718.
38. Huang, Y., Koestner, M. L., and Ackers, G. K. (1996) Heterotropic effects of chloride on the ligation microstates of hemoglobin at constant water activity, *Biophys. J. 71*, 2106−2116.
39. Miyazaki, G., Morimoto, H., Yun, K.-M., Park, S.-Y., Nakagawa, A., Minagawa, H., and Shibayama, N. (1999) Magnesium(II) and zinc(II)-protoporphyrin IX's stabilize the lowest oxygen affinity state of human hemoglobin even more strongly than deoxyheme, *J. Mol. Biol. 292*, 1121−1136.
40. Yun, K.-M., Morimoto, H., and Shibayama, N. (2002) The contribution of the asymmetric $\alpha_1\beta_1$ half-oxygenated intermediate to human hemoglobin cooperativity, *J. Biol. Chem. 277*, 1878−1883.
41. Yonetani, T., Park, S., Tsuneshige, A., Imai, K., and Kanaori, K. (2002) Global allostery model of hemoglobin. Modulation of O_2 affinity, cooperativity, and Bohr effect by heterotropic allosteric effectors, *J. Biol. Chem. 277*, 34508−34520.

BI050709O